

UCSF

UC San Francisco Previously Published Works

Title

A synaptic memory trace for cortical receptive field plasticity.

Permalink

<https://escholarship.org/uc/item/2tb7p591>

Journal

Nature, 450(7168)

ISSN

1476-4687

Authors

Froemke, Robert C
Merzenich, Michael M
Schreiner, Christoph E

Publication Date

2007-11-15

Supplemental Material

<https://escholarship.org/uc/item/2tb7p591#supplemental>

Peer reviewed

Manuscript number: 2006-06-06942D

**A synaptic memory trace
for cortical receptive field plasticity**

Robert C. Froemke*, Michael M. Merzenich & Christoph E. Schreiner

Coleman Memorial Laboratory and
W.M. Keck Foundation Center for Integrative Neuroscience,
Department of Otolaryngology
University of California, San Francisco,
California 94143, USA

* To whom correspondence should be addressed

Phone: 415-476-1762

Fax: 415-476-1941

Email: rfroemke@phy.ucsf.edu

Receptive fields of sensory cortical neurons are plastic, changing in response to alterations of neural activity or sensory experience¹⁻¹². In this way, cortical representations of the sensory environment can incorporate new information about the world, depending on the relevance or value of particular stimuli^{1,6,9}. Neuromodulation is required for cortical plasticity, but it is uncertain how subcortical neuromodulatory systems, such as the cholinergic nucleus basalis (NB), interact with and refine cortical circuits¹³⁻²⁴. Here we determine the dynamics of synaptic receptive field plasticity in the adult primary auditory cortex (AI) using *in vivo* whole-cell recording. Pairing sensory stimulation with NB activation shifted the preferred stimuli of cortical neurons by first inducing a rapid reduction of synaptic inhibition within seconds, followed by a large increase in excitation, both specific to the paired stimulus. Although NB was only stimulated for a few minutes, reorganization of synaptic tuning curves progressed for hours thereafter- inhibition slowly increased in an activity-dependent manner to rebalance the persistent enhancement of excitation, leading to a retuned receptive field with new preference for the paired stimulus. This restricted period of disinhibition may be a fundamental mechanism for receptive field plasticity, and could serve as a memory trace^{9,25} for stimuli or episodes that have acquired new behavioral significance.

A major subcortical nucleus critical for receptive field plasticity is NB, the main source of cortical acetylcholine (ACh)^{4,9,14-17,19-21}. How are neuromodulators such as ACh involved in plasticity, and what circuit elements do they act upon? One possibility is that neuromodulation creates a cellular tag or memory trace for synaptic events that occurred in conjunction with neuromodulator release. However, the effects of ACh on cortical

neurons are diverse, including increased excitability^{19,22,23} and suppression of synaptic transmission^{15,17,23,24}, and it is unclear how these effects could produce long-term response enhancement specific for particular stimuli. Extracellular recordings cannot reveal which cellular events are responsible for receptive field plasticity, and studies *in vitro* do not permit investigation of receptive fields or subcortical interactions with cortical networks. Instead, here we use whole-cell recording and NB stimulation in the intact brain to determine the synaptic basis of cortical receptive field plasticity.

We made *in vivo* whole-cell recordings from adult rat AI (Fig. 1a). Pure tones of different frequencies were played in pseudo-random sequence to the contralateral ear. Frequency tuning was characterized in voltage-clamp at hyperpolarized (-70 mV) and depolarized (-20 mV) levels to reveal tone-evoked excitatory and inhibitory postsynaptic currents (EPSCs and IPSCs), respectively (Fig. 1b).

Before NB pairing, cortical neurons had similar profiles of excitatory and inhibitory frequency tuning, confirming that their levels of excitation and inhibition were balanced^{26,27}. Excitatory and inhibitory tuning curves usually had one shared peak at the best frequency (BF). There was a high correlation between the relative amounts of excitation and inhibition across all frequencies (Supplementary Fig. 1).

After 5-15 minutes of baseline receptive field characterization, a tone was paired repetitively for 2-5 minutes with electrical stimulation of NB (“NB pairing”, Fig. 1b) to release endogenous ACh within AI (although other substances may also be released²⁸). NB was tetanically stimulated (100 Hz, 250 ms) in a manner similar to natural spiking patterns of NB AChergic cells²⁰.

After cessation of NB pairing, we observed large changes to synaptic inputs evoked by the paired tone: pairing rapidly potentiated tone-evoked EPSCs and depressed IPSCs (Fig. 1c,d). Similar results were obtained when conductance and charge transfer were measured (Supplementary Figs. 2 and 3). Synaptic modifications were long lasting and frequency specific (but see below). On average, currents evoked by unpaired tones were not significantly altered, although we consistently observed that responses to the original BF were reduced over a longer time course (Fig. 1d). Thus the main effect of NB pairing is to break the balance between excitation and inhibition at the paired frequency.

Synaptic modifications required paired NB and sensory stimulation. Frequency tuning was not persistently altered when NB was stimulated in silence or when a given tone was repeated without NB stimulation (Supplementary Fig. 4a,b,d). Surprisingly, this was the case even in current-clamp recordings in which tone presentation reliably evoked postsynaptic spikes (Supplementary Fig. 4c,d), demonstrating that repetitive pairing of tones with postsynaptic spikes does not induce long-term potentiation of excitatory postsynaptic potentials (EPSPs) at these synapses.

How do the synaptic modifications observed here correspond to previously reported changes in excitability^{17,22} and spike generation^{4,9,19}? To determine the relation between changes in synaptic input and spike output, we made current-clamp recordings from AI neurons to measure tone-evoked spiking responses before and after NB pairing. Before pairing, tones generally evoked subthreshold EPSPs or a single spike^{26,27,29}. As expected, pairing increased spiking evoked by the paired frequency. This included a dramatic (>7-fold) increase in the probability of firing bursts of 2+ spikes (Supplementary Fig. 5). Consistent with the specific increase in firing rate, pairing had no long-term effect on

input resistance (R_i ; Supplementary Fig. 5b). Thus NB pairing alters the firing mode of cortical neurons, increasing the output of AI to enhance the salience of particular stimuli such as those with new behavioral relevance^{4,9,18} or during periods of increased perceptual demand on attention^{15,30}.

Synaptic modifications and enhancement of spiking occurred not only after NB pairing, but also during pairing itself. To determine the time course of pairing-induced changes, we examined the responses to the paired tone during the pairing procedure (Fig. 2). NB pairing suppressed IPSCs within twenty seconds, but enhancement of EPSCs took approximately three times as long (Fig. 2a-c). Cortical application of atropine, an ACh receptor antagonist, prevented the effects of NB pairing (Fig. 2d)^{9,17}. Therefore, despite the existence of multiple transmitter systems in NB²⁸ and the heterogeneity of ACh modulation^{15,17,19,22-24}, the net effects of NB pairing are suppression of inhibition followed by enhancement of excitation. These results suggest that a central role for NB activation in receptive field plasticity is to trigger spectrotemporally-restricted disinhibition, permissive for induction of Hebbian synaptic plasticity^{1,8,9,11,17}.

We wondered which inputs were modified after NB pairing. The decoupling of inhibition from excitation implied that a primary site of synaptic modification was directly within AI. However, it is unclear to what degree extrinsic or intrinsic projections mediate cortical plasticity^{7,9,11,15,17,24}. To localize the effects of NB pairing, we used an additional pair of stimulation electrodes to concurrently monitor two distinct inputs: one from the ventral division of the thalamic medial geniculate body (MGBv), and one from AI (Fig. 3a). We ensured that both stimulation electrodes were in co-tuned areas by making extracellular recordings of receptive fields through the electrodes.

We initially recorded electrically-evoked synaptic currents by intracortical and thalamic stimulation for 5-10 minutes in absence of sensory stimulation. Then, electrical stimulation was stopped, and NB stimulation was paired with the BF at the sites of thalamic and intracortical stimulation for 2-5 minutes. Finally, sensory and NB stimulation were stopped, and electrical stimulation was resumed (Fig. 3b).

NB pairing persistently modified synaptic currents evoked by intracortical stimulation (Fig. 3c,e) but not thalamic stimulation (Fig. 3d,f). These modifications were similar in sign, magnitude, and duration to changes in tone-evoked synaptic responses. Intracortical EPSCs (cEPSCs) were potentiated, while intracortical IPSCs (cIPSCs) were suppressed (Fig. 3e). Thalamocortical EPSCs (tEPSCs) were unaffected (Fig. 3f), and thalamocortical IPSCs were not observed. These data suggest that NB pairing does not induce strengthening of direct thalamocortical input from neurons of the MGBv tuned to the paired frequency, but it does enhance connections from the region of AI initially tuned to that frequency. The decrease in cIPSC amplitude demonstrates that one location of synaptic modification is directly within AI, at the connections between interneurons and excitatory cells. However, these results do not exclude potential for modification of other synapses elsewhere in the auditory pathway, perhaps on a different time scale or with other requirements for induction^{7,9}.

Finally, we noticed that towards the end of long-term recording sessions (~30 minutes post-pairing; Fig. 1d), IPSCs evoked by tones of the paired frequency seemed to recover back towards their initial amplitudes. This indicated that modification of inhibitory frequency tuning occurred with more complex dynamics than enhancement of excitation. However, as it was difficult to maintain stable recordings for longer than 30+ minutes, we

were unable to follow the complete evolution of inhibitory modifications within individual recordings.

To thoroughly examine the time course of synaptic receptive field plasticity, we made consecutive whole-cell recordings from the same location in AI for hours after NB pairing in each animal (Fig. 4). To compare synaptic modifications across cells, we took advantage of the consistency of frequency tuning for neurons in a given tonotopic region of AI (Supplementary Fig. 1b), and normalized current amplitudes to their maximum values across frequencies.

For example, the recordings shown in Figure 4a-d were each made from the 16 kHz region of AI in the same animal. As expected, BFs of excitation and inhibition for the first recorded neuron were both initially 16 kHz (Fig. 4a, open arrowhead). After pairing NB stimulation with 4 kHz tones, we observed a large increase in the excitation-inhibition ratio (E:I ratio) at the paired frequency (Fig. 4b, arrow). After this recording was finished, we obtained another recording from a second cell in the same location ~100 minutes after pairing (Fig. 4c). The BF of excitation for this cell was 4 kHz, but inhibition was maximal at 8 kHz. Finally, we recorded a third cell, in the same location as the two previous recordings, ~3 hours after pairing (Fig. 4d), and found that BFs of excitation and inhibition were 4 kHz. Thus potentiation of excitation was maintained for hours after transient NB pairing, but after an initial period of suppression, inhibition began to progressively increase until it balanced the enhanced excitation.

Re-establishing a normal E:I ratio required approximately two hours after completion of NB pairing (Fig. 4e, squares). This rebalancing reflects the gradual growth of inhibitory

strength rather than a decrease in excitation at the paired frequency, was apparent for continuously recorded neurons (Fig. 4e, circles), and was registered as shifts in BF (Supplementary Fig. 6). Rebalancing required near-continual tonal stimulation. If auditory stimulation was turned off for 60-90 minutes following NB pairing, suppression of inhibition was maintained and the E:I ratio remained unbalanced (Fig. 4f, “Quiet”). These data are reminiscent of recent findings showing that the timing of the AI critical period can be altered by exposure to different auditory environments^{10,12}.

We have described here a differential progression for changes in cortical excitation and inhibition after NB pairing that reorganizes AI receptive fields. Although NB was stimulated only for a brief period, alteration of excitatory frequency tuning required 30+ minutes to fully manifest, leading to increased preference for paired stimuli. Changes to inhibitory tuning, however, occurred first and continued for hours after NB pairing, eventually increasing to balance the changes in excitation. These results provide a mechanism for the function of NB in attentional modulation: focal disinhibition may act as a synaptic correlate of heightened attentiveness for novel or meaningful stimuli. Furthermore, the long-lasting break in the E:I balance caused by NB pairing maintains the immediate effects of NB activation, allowing restricted parts of cortex to operate in hyperexcitable states independent of further neuromodulation. This transient disinhibition therefore acts as a synaptic memory trace for sensory information of increased significance^{9,25,30}, allowing these stimuli to evoke larger bursts of spikes for a limited time while receptive fields are adjusted to represent the new emphasis for paired inputs.

Methods

Experimental procedures were approved under UCSF IACUC protocols. Experiments were carried out in a sound-attenuating chamber. Female Sprague-Dawley rats 3-5 months old were anesthetized with pentobarbital. A stimulation electrode was implanted in right NB⁴ and right auditory cortex was exposed. Pure tones (0.5-32 kHz, 50 ms duration, 60-80 dB) in pseudo-random sequence were delivered into the left ear canal by a tube sealed to a calibrated speaker. The location of AI was determined by mapping spike responses using tungsten electrodes^{4,12}.

In vivo whole-cell recordings were obtained from AI neurons located 400-1100 μm below the pial surface. Patch pipettes (5-9 $\text{M}\Omega$) contained (in mM): 125 Cs-gluconate, 5 TEACl, 4 MgATP, 0.3 GTP, 10 phosphocreatine, 10 HEPES, 0.5 EGTA, 3.5 QX-314, 2 CsCl, pH 7.2 (voltage-clamp); or: 135 K-gluconate, 5 NaCl, 5 MgATP, 0.3 GTP, 10 phosphocreatine, 10 HEPES, 0.5 EGTA, pH 7.3 (current-clamp). Resting potential: -66.0 ± 10 mV (s.d.); R_i : 105.1 ± 54 $\text{M}\Omega$.

To make consecutive recordings from the same location of AI, subsequent electrodes were positioned at the same penetrations. Currents were normalized to the largest across frequencies, and E:I ratio ($EPSC_{paired}/EPSC_{BF}$)/($IPSC_{paired}/IPSC_{BF}$) was calculated. Frequency tuning was sampled at 0.5-1 octave intervals, outside of the normal variance in BF for a given location in AI.

For microstimulation, stimulation strengths were set at the minimums required (≤ 20 μA) to reliably evoke small synaptic events. Intracortical electrodes were placed 0.4-1 mm from recording electrodes. Thalamic electrodes were implanted in right MGBv.

References

1. Buonomano, D.V. & Merzenich, M.M. Cortical plasticity: from synapses to maps. *Annu Rev Neurosci* **21**, 149-186 (1998).
2. Debanne, D., Shulz, D.E. & Fregnac, Y. Activity-dependent regulation of 'on' and 'off' responses in cat visual cortical receptive fields. *J Physiol* **508**, 523-548 (1998).
3. Gilbert C.D. Adult cortical dynamics. *Physiol Rev* **78**, 467-485 (1998).
4. Kilgard, M.P. & Merzenich, M.M. Cortical map reorganization enabled by nucleus basalis activity. *Science* **279**, 1714-1718 (1998).
5. Chang, E.F. & Merzenich, M.M. Environmental noise retards auditory cortical development. *Science* **300**, 498-502 (2003).
6. Fritz, J., Shamma, S., Elhilali, M. & Klein, D. Rapid task-related plasticity of spectrotemporal receptive fields in primary auditory cortex. *Nat Neurosci* **6**, 1216-1223 (2003).
7. Suga, N. & Ma, X. Multiparametric corticofugal modulation and plasticity in the auditory system. *Nat Rev Neurosci* **4**, 783-794 (2003).
8. Malenka, R.C. & Bear, M.F. LTP and LTD: an embarrassment of riches. *Neuron* **44**, 5-21 (2004).
9. Weinberger, N.M. Specific long-term memory traces in primary auditory cortex. *Nat Rev Neurosci* **5**, 279-290 (2004).
10. Chang, E.F., Bao, S., Imaizumi, K., Schreiner, C.E. & Merzenich, M.M. Development of spectral and temporal response selectivity in the auditory cortex. *Proc Natl Acad Sci USA* **102**, 16460-16465 (2005).
11. Karmarkar, U.R. & Dan, Y. Experience-dependent plasticity in adult visual cortex.

Neuron **52**, 577-585 (2006).

12. de Villers-Sidani, E., Chang, E.F., Bao, S. & Merzenich, M.M. Critical period window for spectral tuning defined in the primary auditory cortex (A1) in the rat. *J Neurosci* **27**, 180-189 (2007).

13. Bear, M.F. & Singer, W. Modulation of visual cortical plasticity by acetylcholine and noradrenaline. *Nature* **320**, 172-176 (1986).

14. Everitt, B.J. & Robbins, T.W. Central cholinergic systems and cognition. *Annu Rev Psychol* **48**, 649-684 (1997).

15. Sarter, M., Hasselmo, M.E., Bruno, J.P. & Givens, B. Unraveling the attentional functions of cortical cholinergic inputs: interactions between signal-driven and cognitive modulation of signal detection. *Brain Res Brain Res Rev* **48**, 98-111 (2005).

16. Zhang, Y., Hamilton, S.E., Nathanson, N.M. & Yan, J. Decreased input-specific plasticity of the auditory cortex in mice lacking M1 muscarinic acetylcholine receptors. *Cereb Cortex* **16**, 1258-1265 (2006).

17. Rasmusson, D.D. The role of acetylcholine in cortical synaptic plasticity. *Behav Brain Res* **115**, 205-218 (2000).

18. Yu, A.J. & Dayan, P. Uncertainty, neuromodulation, and attention. *Neuron* **46**, 681-692 (2005).

19. Metherate, R., Cox, C.L. & Ashe, J.H. Cellular bases of neocortical activation: modulation of neural oscillations by the nucleus basalis and endogenous acetylcholine. *J Neurosci* **12**, 4701-4711 (1992).

20. Lee, M.G., Hassani, O.K., Alonso, A. & Jones, B.E. Cholinergic basal forebrain neurons burst with theta during waking and paradoxical sleep. *J Neurosci* **25**, 4365-4369

(2005).

21. Richardson, R.T. & DeLong, M.R. A reappraisal of the functions of the nucleus basalis of Meynert. *Trends Neurosci* **11**, 264-267 (1988).

22. Woody, C.D. & Gruen, E. Acetylcholine reduces net outward currents measured in vivo with single electrode voltage clamp techniques in neurons of the motor cortex of cats. *Brain Res* **424**, 193-198 (1987).

23. Xiang, Z., Huguenard, J.R. & Prince, D.A. Cholinergic switching within neocortical inhibitory networks. *Science* **281**, 985-988 (1998).

24. Metherate, R., *et al.* Spectral integration in auditory cortex: mechanisms and modulation. *Hear Res* **206**, 146-158 (2005).

25. Thompson, R.F. In search of memory traces. *Annu Rev Psychol* **56**, 1-23 (2005).

26. Wehr, M. & Zador, A.M. Balanced inhibition underlies tuning and sharpens spike timing in auditory cortex. *Nature* **426**, 442-446 (2003).

27. Tan, A.Y.Y., Zhang, L.I., Merzenich, M.M. & Schreiner, C.E. Tone-evoked excitatory and inhibitory synaptic conductances of primary auditory cortex neurons. *J Neurophysiol* **92**, 630-643 (2004).

28. Gritti, I., Manns, I.D., Mainville, L. & Jones, B.E. Parvalbumin, calbindin, or calretinin in cortically projecting and GABAergic, cholinergic, or glutamatergic basal forebrain neurons of the rat. *J Comp Neurol* **458**, 11-31 (2003).

29. DeWeese, M.R., Wehr, M. & Zador, A.M. Binary spiking in auditory cortex. *J Neurosci* **23**, 7940-7949 (2003).

30. Hromadka, T. & Zador, A.M. Towards the mechanisms of auditory attention. *Hear Res* **229**, 180-185 (2007).

Supplementary Information is linked to the online version of the paper at www.nature.com/nature.

Acknowledgements:

We thank K.L. Arendt, T. Babcock, Y. Dan, E. de Villers-Sidani, M.R. DeWeese, M.P. Kilgard, D. Polley, L. Wilbrecht, and J.A. Winer for comments and discussions, and S. Bao, W. Huang, K. Imaizumi, A. Tan, and C.-L. Teng for technical assistance. D. Bliss created the artwork in Figs. 1a and 4a. This work was supported by the NIDCD, the Conte Center for Neuroscience Research at UCSF, Hearing Research Inc., and the John C. and Edward Coleman Fund. R.C.F. is a recipient of the Jane Coffin Childs Postdoctoral Research Fellowship and the Sandler Translational Research Fellowship.

Competing interests statement:

The authors declare that they have no competing financial interests.

Figure Legends

Figure 1. Synaptic modifications induced by NB pairing. **a**, Experimental configuration. **b**, Experimental procedure. **c**, Example of pairing-induced modification of synaptic tuning curves. Top, excitatory tuning. EPSCs at the paired frequency (2 kHz) increased from -54.9 ± 10.9 to -92.4 ± 6.6 pA (68.4%, $p < 0.006$, t-test; filled symbols). Lines, tuning before (dashed gray) and ~10 minutes after (solid black) pairing. Arrow, paired tone. Bottom, inhibitory tuning. IPSCs at the paired frequency decreased from 67.6 ± 15.2 to 27.0 ± 7.4 pA (-60.1% , $p < 0.03$; open symbols). **d**, Time course. Top, paired frequency (excitation: $68.0 \pm 13.9\%$, $n=15$, $p < 0.0007$; inhibition: $-24.8 \pm 6.0\%$, $p < 0.0002$). Horizontal bar, NB pairing. Center, original BF. Bottom, other unpaired tones. Error bars, s.e.m.

Figure 2. Rapid suppression of inhibition during NB pairing. **a**, IPSCs decreased from 55.7 ± 2 to 32.3 ± 4 pA (-41.9% , $p < 0.002$) 41-60 seconds after pairing. Solid line, NB pairing. Dashed line, mean current before pairing. **b**, EPSCs increased from -49.5 ± 3 to -70.3 ± 5 pA (42.0%, $p < 0.01$). **c**, Suppression of inhibition occurred before enhancement of excitation (inhibition: 20.7 ± 9.3 seconds, excitation: 52.4 ± 4.1 seconds, $p < 0.009$). Filled symbols, excitation (1-20 seconds: $6.5 \pm 8.6\%$, $n=9$, $p > 0.4$; 41-60 seconds: $29.8 \pm 2.2\%$, $p < 0.003$); open symbols, inhibition (1-20 seconds: $-24.5 \pm 3.8\%$, $n=6$, $p < 0.005$; 41-60 seconds: $-28.1 \pm 7.0\%$, $p < 0.02$). **d**, Atropine (1 mM) blocked the effects of NB pairing ($n=4$, $p > 0.5$). Error bars, s.e.m.

Figure 3. NB pairing altered intracortical connections. **a**, Experimental configuration. **b**, Experimental procedure. **c**, Intracortical stimulation. Left, receptive field recorded with stimulation electrode (16 kHz region of AI). Right, whole-cell recording from 6 kHz region of AI, before (gray) and after (black) pairing NB stimulation with 16 kHz tones. cEPSCs increased (73.4%; $p < 0.03$) and cIPSCs decreased (-47.1%; $p < 0.03$). **d**, Same experiment as **c**, but thalamic stimulation. tEPSCs were unchanged ($p > 0.5$). **e**, NB pairing enhanced cEPSCs ($72.8 \pm 20.5\%$, $n=7$, $p < 0.02$; filled) and suppressed cIPSCs ($-30.7 \pm 3.6\%$, $p < 0.004$; open). **f**, Same experiments as **e**, but for tEPSCs ($p > 0.4$). Error bars, s.e.m.

Figure 4. Temporal dynamics of synaptic receptive field plasticity. **a**, Frequency tuning before pairing. Arrow, paired frequency (4 kHz; E:I ratio: 0.9). Arrowhead, original BF (16 kHz). **b**, Same cell as **a**, 30 minutes post-pairing (E:I ratio: 1.78). **c**, Second cell, 100 minutes post-pairing (E:I ratio: 1.18). **d**, Third cell, 180 minutes post-pairing (E:I ratio: 1.0). **e**, Rebalance of E:I ratio at paired frequency. Squares, consecutive recordings from cell populations at the same locations (“Pop.”). Dashed line, exponential fit. Circles, individual continuous recordings from Fig. 1d (“Indiv.”). **f**, E:I ratio 90-120 minutes post-pairing (“Tones”, E:I ratio increase of $7.5 \pm 6.9\%$, $n=12$; “Quiet”, E:I ratio increase of $44.6 \pm 7.9\%$, $n=6$, $p < 0.004$). Double asterisks, $p < 0.01$. Error bars, s.e.m.

Online Methods

Surgical preparation. All experimental procedures used in this study were approved under UCSF IACUC protocols. Experiments were carried out in a sound-attenuating chamber. Female Sprague-Dawley rats 3-5 months old and weighing 260-350 g were anesthetized with pentobarbital. A bipolar stimulation electrode (Rhodes) was implanted in the right nucleus basalis (stereotaxic coordinates from bregma, in mm: 2.3 posterior, 3.3 lateral, 7 ventral)⁴ and the right auditory cortex was exposed. Localization and stimulation strength (50-200 μ A) were determined by EEG desynchronization (decrease in 1-10 Hz power: $-35.9\pm 2.0\%$, increase in 25-60 Hz power: $65.8\pm 8.9\%$). Pure tones (0.5-32 kHz at 0.5-1 octave intervals, 50 ms duration, 60-80 dB intensity, 0.5 Hz rate) in pseudo-random sequence were delivered into the left ear canal by a tube sealed to a calibrated speaker. The location of AI was determined by mapping multiunit spike responses at 500-700 μ m below the surface using parylene-coated tungsten electrodes: AI neurons spike at short latency (8-16 ms) to the best frequency and are tonotopically organized from high to low frequency along the anterior-posterior axis^{4,12}.

Whole-cell recording. *In vivo* whole-cell recordings were obtained from neurons located 400-1100 μ m below the pial surface (mean depth of 773 ± 191 μ m, s.d.); there was little correlation between recording depth and changes induced by NB pairing to either excitation (r : 0.1, $p>0.7$) or inhibition (r : -0.3 , $p>0.3$). Cortical pulsations were prevented with 4% agar. Recordings were made with an AxoClamp 2B (Molecular Devices). For voltage-clamp recording, patch pipettes (5-9 M Ω) contained (in mM): 125 Cs-gluconate, 5 TEACl, 4 MgATP, 0.3 GTP, 10 phosphocreatine, 10 HEPES, 0.5 EGTA, 3.5 QX-314,

2 CsCl, pH 7.2. For current-clamp recording, pipettes contained: 135 K-gluconate, 5 NaCl, 5 MgATP, 0.3 GTP, 10 phosphocreatine, 10 HEPES, 0.5 EGTA, pH 7.3. Mean resting potential: -66.0 ± 10 mV (s.d.); series resistance (R_s): 24.8 ± 6 M Ω ; R_i : 105.1 ± 54 M Ω . Cells were excluded if R_i or R_s changed $>30\%$ over the entire experiment^{31,32}. Data were filtered at 2 kHz, digitized at 10 kHz, and analyzed with Clampfit 10 (Molecular Devices) and Matlab 6 (MathWorks).

For voltage-clamp experiments, we measured peak current amplitudes at -70 mV and -20 mV, near the reversal potentials for outward and inward currents, respectively. Excitation was measured as the mean of a 1-2 msec window centered on the peak (~ 10 -20 msec after tone onset); inhibition was measured as the mean of a 10 msec window ~ 25 -40 msec after tone onset. While PSCs contain a mixture of excitatory and inhibitory input, and excitatory currents are not completely cancelled at -20 mV, the residual inward currents that remained were clearly separated in time from outward currents²⁷. We used previously published methods to measure synaptic conductances^{26,27}. Charge transfer was measured over 10-70 msec after tone onset. For current-clamp experiments (Supplementary Figs. 4,5), we measured synaptic strength as the first 2 ms of the EPSP slope³¹. A ‘burst’ of spikes was defined as two or more spikes with an inter-spike interval of <10 ms.

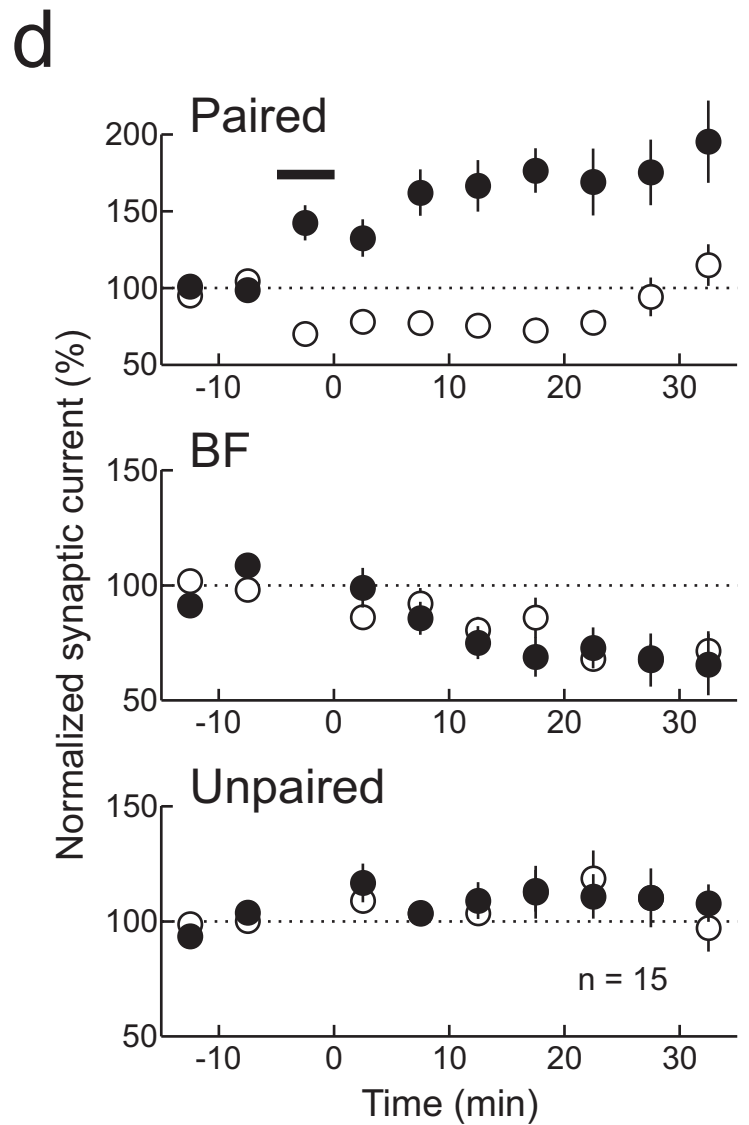
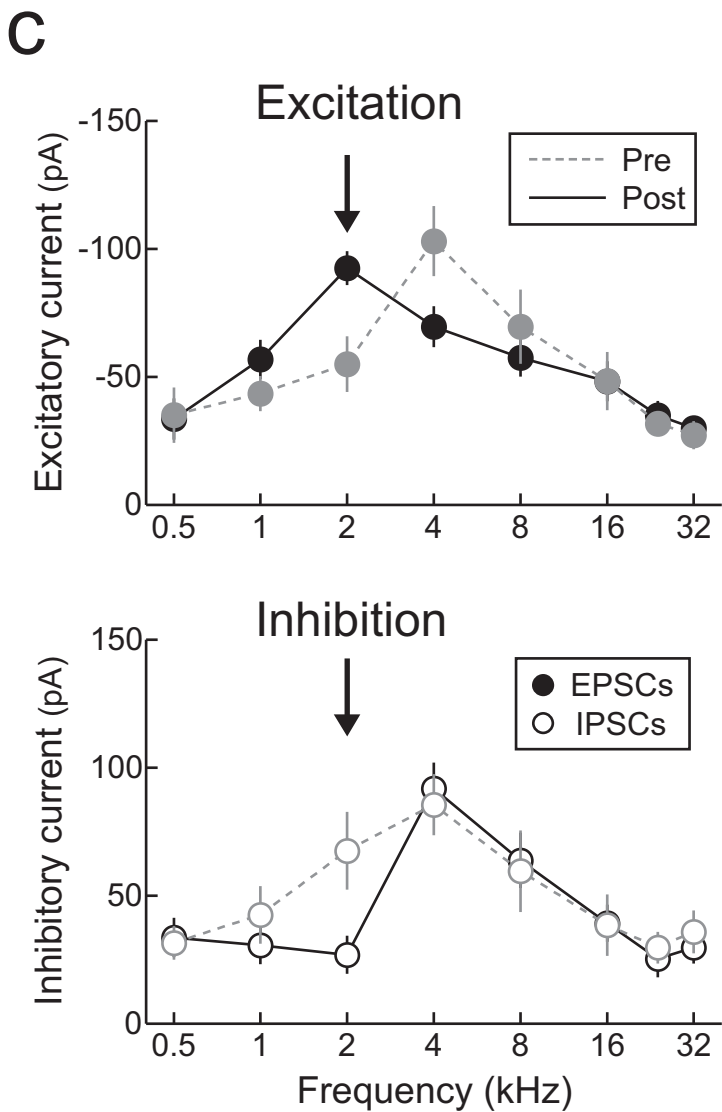
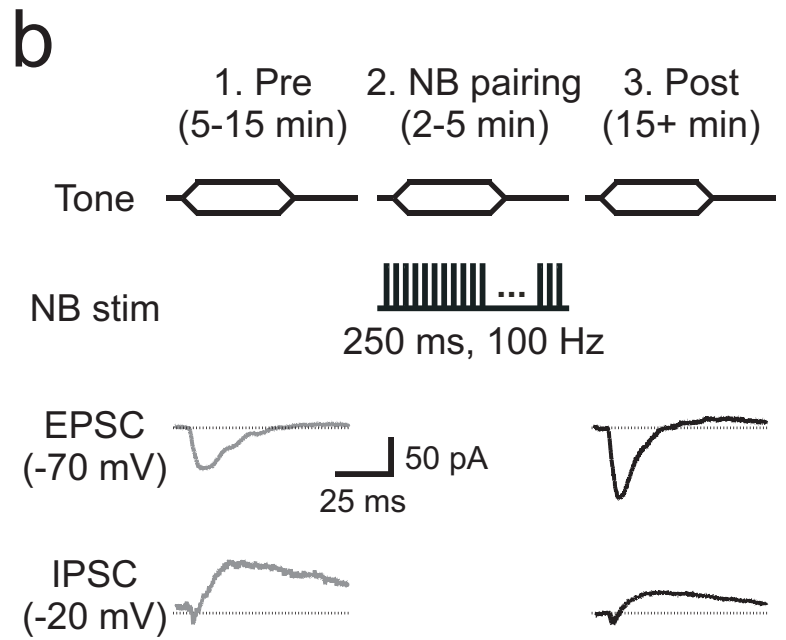
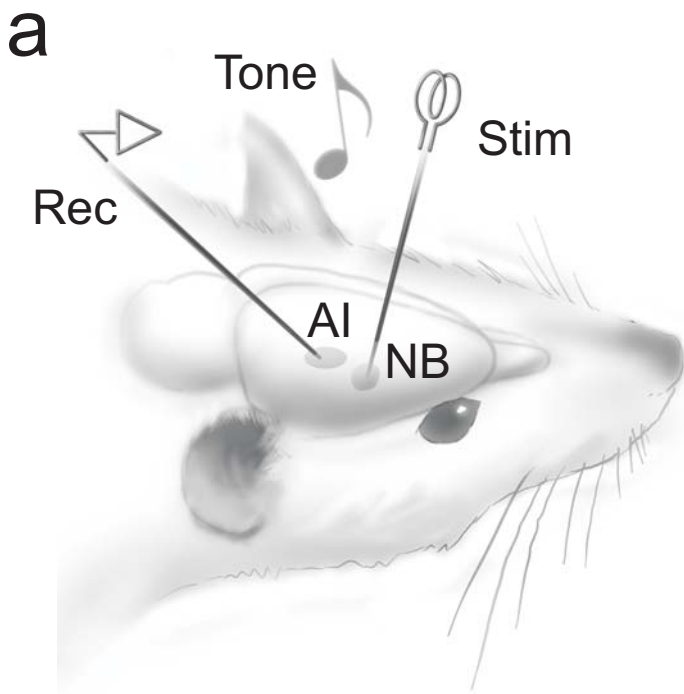
For microstimulation experiments (Fig. 3), tungsten electrodes (0.7-1.3 M Ω) were used, and stimulation strengths (0.1-20 μ A, 0.1-1 ms) were set at the minimum intensity required to reliably evoke small synaptic events (average peak amplitudes: cEPSCs, -14.0 ± 3.3 pA; cIPSCs, 11.7 ± 3.9 pA; tEPSCs, -24.7 ± 6.7 pA; s.d.). The intracortical

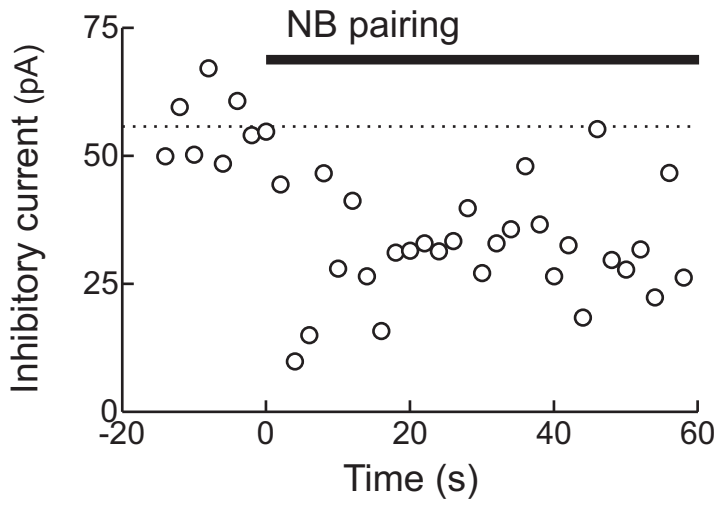
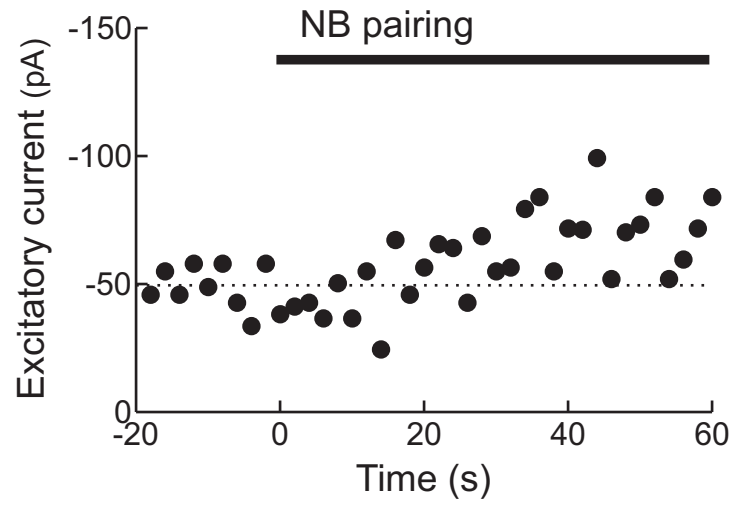
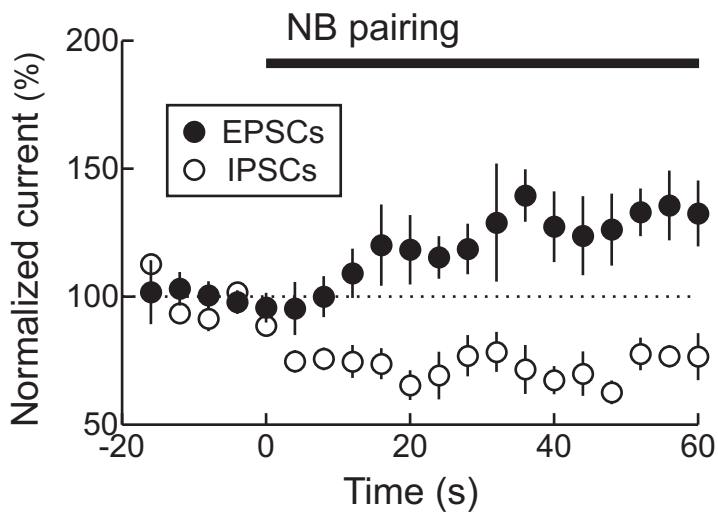
electrode was placed 0.4-1.0 mm from the recording electrode at a depth of ~1 mm (layer V). The thalamic electrode was implanted in the ipsilateral MGBv (from bregma, in mm: 5.8 posterior, 3.5 lateral, 5-6 ventral). Cortical and thalamic electrodes evoked responses from separate inputs, as determined by the linear summation of synaptic currents evoked from both sources simultaneously (measured/predicted EPSC summation ratio: $98 \pm 3\%$, $p > 0.5$).

To make consecutive recordings from the same location of AI (Fig. 4 and Supplementary Fig. 6 online), subsequent recording electrodes were positioned at the same cortical penetration as the first electrode. We estimate our error in electrode positions to be $< 100 \mu\text{m}$. Single-unit recordings from AI have demonstrated some local variation in best frequency among nearby neurons, with mean scatter of 0.33 octaves³³. In the present study, however, frequency tuning was sampled at 0.5-1 octave intervals, outside of the normal variance in preferred frequency for a given location in AI. Currents were normalized to the largest across frequencies, and E:I ratio ($EPSC_{paired}/EPSC_{BF})/(IPSC_{paired}/IPSC_{BF})$ was calculated.

References

31. Froemke, R.C., Tsay, I.A., Raad, M., Long, J.D., & Dan, Y. Contribution of individual spikes in burst-induced long-term synaptic modification. *J Neurophysiol* **95**, 1620-1629 (2006).
32. Meliza, C.D. & Dan, Y. Receptive-field modification in rat visual cortex induced by paired visual stimulation and single-cell spiking. *Neuron* **49**, 183-189 (2006).
33. Schreiner, C.E. & Sutter, M.L. Topography of excitatory bandwidth in cat primary auditory cortex: single-neuron versus multiple-neuron recordings. *J Neurophysiol* **68**, 1487-1502 (1992).



a**b****c****d**